aerospace

MDPI

Article

Path Planning of Multiple Unmanned Aerial Vehicles Covering Multiple Regions Based on Minimum Consumption Ratio

Jian Chen [1,2], Ruikang Zhang [1], Hongqiang Zhao [1], Jiejie Li [1,*] and Jilin He [1,3,*]

[1] College of Mechanical and Electrical Engineering, Central South University, Changsha 410083, China
[2] State Key Laboratory of Fluid Power and Mechatronic Systems, Zhejiang University, Hangzhou 310027, China
[3] Hunan Sunward Technology Co., Ltd., Changsha 412002, China
* Correspondence: jiejieli@csu.edu.cn (J.L.); hejilin@csu.edu.cn (J.H.)

Abstract: Investigating the path planning of multiple unmanned aerial vehicles (UAVs) covering multiple regions, this work proposes an effective heuristic method of region coverage path planning to reduce the complexity of the problem. The proposed method decomposes the solution process into two stages. First of all, the two most important parameters affecting the performance of UAV missions were considered, namely, the flying speed and the scan width. According to these two parameters of UAVs, a new multi-regional allocation scheme based on the minimum consumption ratio was proposed. With this allocation scheme, the coverage task allocation and path pre-planning of UAVs were obtained. Then, the UAVs' trajectory routes were optimized based on the dynamic planning algorithm to reduce the time consumption of UAVs on the transfer path between regions. The method was evaluated with numerical experiments. The results showed that the proposed method can effectively solve the path planning problem of multiple UAVs covering multiple regions. Compared with an advanced algorithm, the time consumption for homogeneous and heterogenous UAV performance was reduced by 5.1% and 3%, respectively.

Keywords: UAV; region allocation; dynamic planning; path planning; minimum consumption ratio

Citation: Chen, J.; Zhang, R.; Zhao, H.; Li, J.; He, J. Path Planning of Multiple Unmanned Aerial Vehicles Covering Multiple Regions Based on Minimum Consumption Ratio. *Aerospace* **2023**, *10*, 93. https://doi.org/10.3390/aerospace10020093

Academic Editor: Hailong Huang

Received: 13 December 2022
Revised: 13 January 2023
Accepted: 13 January 2023
Published: 17 January 2023

1. Introduction

With the improvement and development of unmanned aerial vehicle (UAV) technology, UAVs have become widely used in a growing number of scenarios. Due to their advantages of having a low cost, small size and low risk, UAVs have an irreplaceable role in both military [1] and civilian [2,3] applications. However, the requirements of many practical applications are beyond the capability of a single UAV due to the limitations of endurance, communication bandwidth and sensing range. Compared with the single UAV, the multi-UAV system has high concurrency and robustness. The collaboration of multiple UAVs can achieve higher efficiency [4]. Coverage path planning (CPP) is one of the key research fields in multi-UAV application, which is significant in the application of UAVs. The mobile target coverage is suitable for mobile military unit tracking or monitor sensor tracking, which was well researched by Huang et al. [5]. In comparison, the stationary multi-regional coverage is more suitable for regional observations or reconnaissance, such as in battlefield reconnaissance, disaster rescue, civil exploration, agriculture and mapping [6], particularly for spraying pesticides in farms [7] or monitoring forest fires [8]. Therefore, the research on CPP for UAVs is significant for broadening the application of UAVs and bringing more benefits in many fields.

In stationary multi-regional coverage, the specific requirements and constraints vary case by case. For example, in the application of pesticides, the UAV is required to fly within the farm region so that the pesticides will not pollute other lands [9]. UAVs are also constrained by endurance depending on the batteries or fuel carried [10]. In this situation, the minimum distance is normally the optimizing target.

In this study, the minimum consumption time was the target for optimization. Reasonably allocating regions to each UAV was the key to the optimization. Since heterogenous UAVs have different flying speeds, the minimum time cannot be deduced directly from minimum distance. To achieve the minimum time, an efficient heuristic based on the minimum consumption ratio (MCR) was proposed. Based on the UAVs' flying speed and scan width, the CPP model was established, and an exact formulation based on mixed-integer linear programming was given. Consequently, a region allocation method based on the MCR was developed. Then, the transfer path of each UAV was reconstructed by combining with a dynamic programming algorithm. According to the proposed model and method, different algorithms, different numbers of drones and different numbers of regions were set up for numerically experimental verification. The comparison results showed the proposed method in this study had obvious improvement of CPP. The main contribution of this study is the utilization of the MCR to allocate the regions to UAVs more reasonably. Additionally, applying dynamic programming reconstructed the CPP and achieved a shorter consumption time. These contributions enriched the theoretical basis of this field and provided more opportunities for UAV application.

2. Related Works

CPP can include either a single region or multiple regions. A large number of studies on regional CPP can be found for single-region CPP, as shown in Figure 1a. Random coverage [11], roundabout coverage [12] and spiral coverage [13] as well as certain plane-filling curves, such as the Peano curve and Moore curve [14], were commonly used in the full coverage of a single region. The popular algorithm in single-region path planning included genetic algorithm [15,16], biased random key genetic algorithm [17], two-tie search algorithm [18], the interlaced back-and-forth pattern [19], grid-based algorithm to reduce/minimize energy consumption [20,21], machine learning to maximize efficiency [22], ant colony optimization (ACO) algorithm [23], etc. Some algorithms were also adapted to path planning of multi-UAV for a single region. For example, grid cells were used to discretize the detecting region, dividing it into subdomains, and transforming the problem into a single UAV problem [24]. The neural network approach was also applied to multi-robot CPP where the robots were treated as moving obstacles in each other [25]. The method on robots CPP is also adaptive to 2D CPP for UAVs [26].

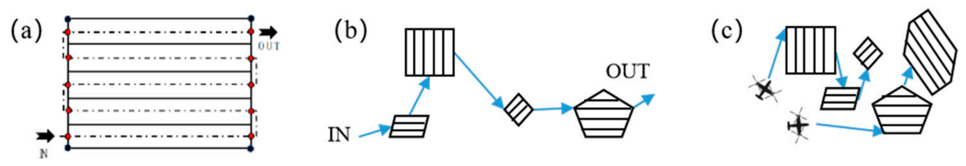

Figure 1. Coverage path planning: (**a**) single region; (**b**) multiple regions for single UAV; (**c**) multiple regions for multiple UAVs.

As for single UAV coverage path planning for multiple regions in Figure 1b, the problem can be regarded as a traveling salesman problem (TSP). The TSP has been well researched and many accurate solution methods are available, including the classical heuristic solution method, the intelligent optimization method [27,28] and memory-enhanced dueling deep Q network [29]. Therefore, research in this field will not be discussed here.

In comparison, CPP of multiple regions for multiple UAV collaboration shown in Figure 1c was lacking research interest. This problem is an NP-hard problem [30]. The difficulty of solving it explodes as the number increases. Therefore, the problem was normally solved by two steps: region allocation and path planning. The heuristic solution is the key to solving the coverage of multi-UAVs cooperative region. When neglecting the path planning within regions, the regions can be treated as points and the linear-programming-based formulation can achieve the basic region allocation. Then, the ACO can be applied to seek the optimal path for each UAV to cover these regions [31]. The ACO was also successfully applied to solve the CPP problem of 3D urban environments including avoiding obstacles [32]. A heuristic solution method based on the high effective time rate first (HETRF) was proposed [33]. The results showed significant improvement when compared with the results from large-region-first scheduling, short-distance-first scheduling and the highest-effective-time-ratio-first method [33]. In the HETRF algorithm, the time spent scanning regions was defined as effective time. Therefore, the effective time ratio, which was defined as the ratio of effective time to the total time, was the target of optimization. This research was extended as further consideration of energy constraint in the CPP [34]. Similarly, a balanced effective task rate (BETR) algorithm was proposed to balance the working time spent in large regions and small regions [35]. In BETR, the large regions were given priority. Then, a variational ACO was applied to adjust the travel orders. Another study implemented mixed-integer linear programming formulations to determine a route for each vehicle with a minimum total cost, and this method was transferable for the CPP problem of UAVs [36]. A clustering-based algorithm was proposed to classify regions into clusters to minimize the finishing time after the flight path allocation by the mixed-integer linear programming [37]. To accurately calculate the route time spent for each UAV, the turning time during the UAV changing path was also considered by Li et al.'s work [38].

3. Problem Formulation

As discussed above, the CPP problem can be treated as an NP-hard problem. This problem has also been described in previous research [22,23]. Based on these descriptions, this study aims to optimize the time consumption of finishing tasks. The multi-region coverage problem can be described as follows. UAVs carrying cameras scan all the regions. The finishing time is the last UAV finishing the last region. For a set of UAVs with different speeds and scan camera performances, $U = \{U_1, U_2, \dots, U_n\}$, where n is the number of UAVs, and the m regions that need to be covered are $R = \{R_1, R_2, \dots, R_m\}$. The corresponding regions' areas are $A = \{a_1, a_2, \dots, a_m\}$. The distance between regions cannot be ignored due to large distance between R_i and R_j. The distance between any two regions is expressed by d_{ij}. All drones take off from the base site to cover the target regions, giving the shortest time for completing the task of covering all target regions.

Some assumptions were made in this study. (1) As shown in Figure 2, the overall region was a 2D plane and there were no obstacles in the 2D plane. (2) The detailed path planning in every single target region was not specified. The path for scanning in every single path started from the center and went through the divided grids generated by the spanning trees without repetition. (3) The entry point and exit point were assumed to be the center of the target region. (4) The endurance of UAVs was assumed to meet the requirements of each path.

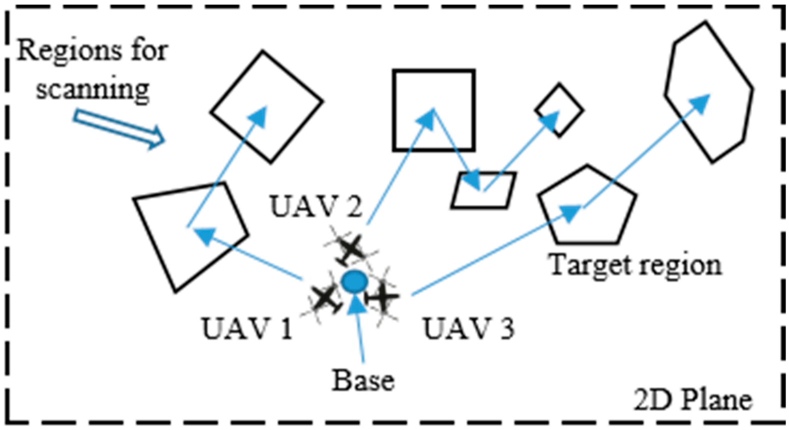

Figure 2. The problem description of multi-regional CPP for multiple UAVs.

The flight speed of the UAVs and the performance of the scan camera are the two main parameters influencing the time it takes to finish the mission. The performance of UAV i was set as $U_i = [v_i, w_i]$, where v_i and w_i are the speed and scan width of UAV i. The scan width w shown in Figure 3 can be found in

$$w = w_1 = \frac{2htan\frac{\beta}{2}}{\sin\left(\alpha - \theta + \gamma\right)} \tag{1}$$

where h is the height of the UAV from the ground, α is the mounting angle of the UAV imaging sensor, β is the rear horizontal field of view angle (rear horizontal angle of view) and δ is the front horizontal angle of view, γ is the vertical field of view angle (vertical field of view) of the UAV imaging sensor, θ is the elevation angle of the UAV, w_1 is the rear width of the scan area and w_2 is the front width of the UAV scanning area. To simplify the problem, h, α, β, δ, γ and θ were assumed constant and scan width w is set to a fixed value. For the UAV performing the coverage task, the efficiency of the full coverage mission is affected by the scanning width of the UAV, w, which was defined as the scanning capability of the UAV.

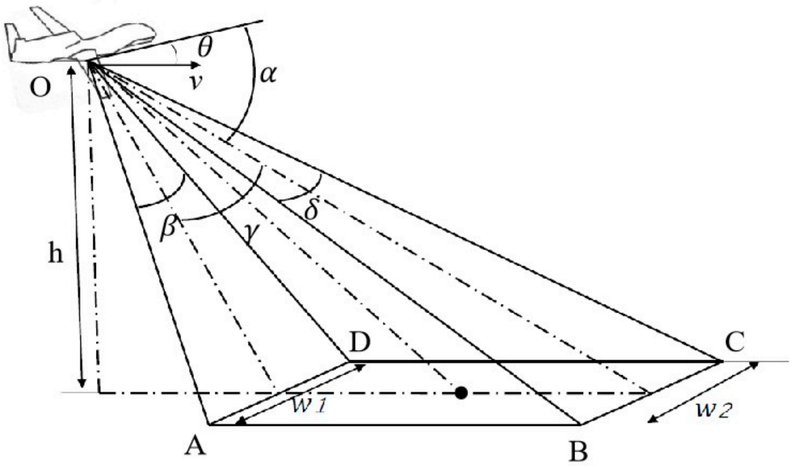

Figure 3. The scan width of UAVs.

Define x_{ij}^k and x_j^k as

$$x_{ij}^k = \begin{cases} 1, & U_k\,fly\,from\,R_i\,to\,R_j \\ 0, & others \end{cases} \tag{2}$$

$$x_j^k = \begin{cases} 1, & U_k\ covered\ R_j \\ 0, & others \end{cases} \tag{3}$$

The objective function can be defined as

$$\min_{1 \le k \le n} \left\{ max \left\{ \sum_{i=0}^{m} \sum_{j=1}^{m} \frac{d_{ij}}{v_k} x_{ij}^k + \frac{a_j}{v_k w_k} x_j^k \right\} \right\} \tag{4}$$

subject to

$$\sum_{j=1}^{m} \sum_{k=1}^{n} x_{0j}^k = n \tag{5}$$

$$\sum_{j=1}^{m} \sum_{k=1}^{n} x_{ij}^k = 1, i = 1,2, \ldots, m \tag{6}$$

$$\sum_{i=0}^{m} \sum_{k=1}^{n} x_{ij}^k = 1, j = 1,2, \ldots, m \tag{7}$$

$$\sum_{k=1}^{n} x_j^k = 1, j = 1,2, \ldots, m \tag{8}$$

where d_{ij} is the distance between R_i and R_j. Equation (5) ensures that the number of UAVs taking off from the base is n. Equations (6)–(8) ensure that each region will be visited once.

4. Methodology

4.1. Minimum Consumption Ratio for Coverage Path Planning

According to the characteristics of this problem, the solution included two stages. First, the region allocation was conducted according to the UAV performance, mission area and transfer distance between regions. Then, the transfer path of each UAV was optimized to realize the coordinated coverage of all regions. For solution convenience, in this paper, the distance between the regions is represented by the linear distance at the center of the region, which is the distance equivalent to the transfer path between the regions.

The performance of the drone partly determined how many tasks it is assigned. The UAV will preferentially select close and large areas for coverage to enable the UAV to complete the coverage task as soon as possible. However, in practical situations, the large areas may not be close. Therefore, this paper proposed a region distribution method to balance both the flying distance and the target area.

The conception of effective time was also implemented in this study. The UAV on the coverage path when covering the target area was defined as effective time consumption. In this paper, the specific coverage path in one region is not discussed in depth. When covering a region, each UAV started from the region center and went through the divided grids generated by the spanning trees without repetition. The UAV returned to the region center after completing the separate region coverage. Therefore, the consumed time in separating regions can be expressed as $\frac{a_j}{v_k w_k}$. The traveling time between regions was defined as ineffective time consumption and can be calculated by $\frac{d_{ij}}{v_k}$. Therefore, the aim of region allocation became seeking a coverage method to make ineffective consumption as small as possible. The ratio of the ineffective consumption to effective consumption was used to quantify the ineffective consumption in the overall mission. For all unvisited regions, the UAV preferentially selected the region quantified by a minimum consumption ratio (MCR) to cover.

Additionally, to avoid the problem of large difference in the coverage time of each UAV caused by the larger region, the larger region is given priority, so the region selection coefficient is introduced as

$$q = \frac{A}{a_j}\ j = 1,2, \ldots, m; (0 < \frac{1}{q} < 1\ and\ \sum_{j=1}^{m} \frac{1}{q_j} = 1) \tag{9}$$

Then, the MCR for R_j to UAV in R_i was

$$MCR_j = q \times \frac{d_{ij}}{v_k} \div \frac{a_j}{v_k w_k} = \frac{A d_{ij} w_k}{a_j^2} \tag{10}$$

In this regional CPP problem, the longest UAV mission time cost was the total time for all UAVs to complete the coverage task. When assigning tasks to the drone, the time cost of each drone should be as close to equal as possible. After assigning the first area to each drone, the drone which completed the current coverage task had the priority to the next area. Areas were alternately assigned to each UAV according to the MCR principle until all area allocation was completed. The MCR algorithm is shown below.

Through Algorithm 1, the UAV achieved the reasonable allocation of full coverage tasks in irregular target areas. It provided support for the UAV to complete the coverage task in the shortest time.

Algorithm 1 Minimum Consumption Ratio Algorithm

Input: UAV set: $U = \{U_1, U_2, \dots, U_n\}$; Target Regions set: $R = \{R_1, R_2, \dots, R_m\}$.
Output: Set of mission areas for each UAV

```
Number the UAVs according to the coverage capability from small to large
Initialize region accessible variable v[m] ← 1
Initialize the number of regions variable k = 0
While b < m do
    U_b ← the first drone completes covering the current mission area
    for i = 1 to m do
      if (v[m] ≠ 0) then
            Calculate the MCR of the corresponding node r_i for U_b
    end if
    end for
Select the region with an MCR and labeled as r_j
v[j] ← 0
b ← b + 1
end while
```

4.2. Coverage Path Replanning by Dynamic Planning

On the basis of the first stage, it is necessary to minimize the consumption of the UAV on the flight path to further improve the time efficiency. The path optimization can be treated as traversing all the scattered target regions without returning to the starting point. To address this problem, a method of dynamic planning was applied.

Set all vertices as V. With some vertices V', $D(x, V')$ represented the shortest distance from the starting point s, passing all target points in V' once and arriving at x. The distance from point x to y was represented by $C_{x \to y}$. In the initial state, the minimum flying distance starting from point s without passing any other vertices is zero. Namely, the initial state equation can be expressed as

$$D(s, \{s\}) = 0 \tag{11}$$

If the drone arrived at point q and the next point was z, then the distance from s to point z can be represented by $D(q, V') + C_{q \to z}$. The state transfer equation can be expressed as

$$D(z, V' + z) = \min\{D(q, V') + C_{q \to z}\}, q \in V' \tag{12}$$

The objective function $Minlen$ for solving the shortest distance can be obtained as Equation (13).

$$Minlen = \min\{D(x, V)\}, x \in V \quad (13)$$

The flow chart of the dynamic planning algorithm is shown in Figure 4. The algorithm obtained the traversal order and the shortest distance length on the transfer path.

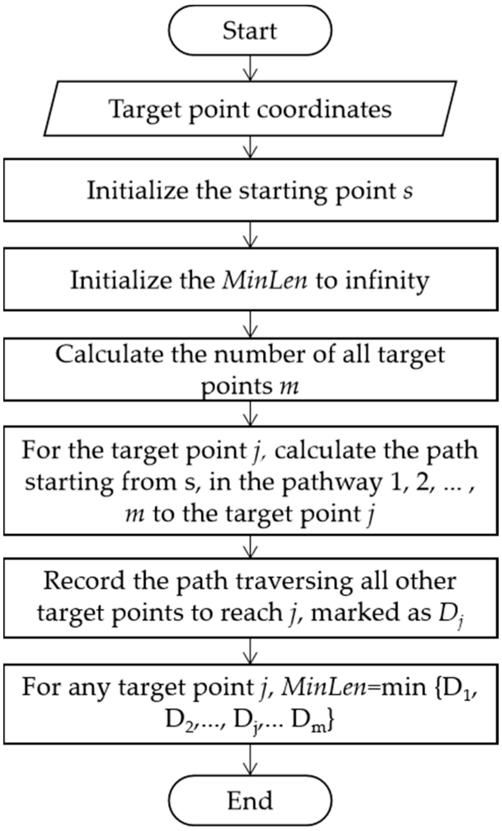

Figure 4. Flow chart of the path replanning algorithm.

5. Numerical Experiments

Numerical experiments on full-coverage CPP of multi-UAV and multi-region based on MCR task allocation algorithm was conducted.

The configuration for computing numerical experiments was Intel(R) Core(TM) i5-9300M CPU 2.40GHz with 16GB of system memory. The code was written in C++.

Experimental scenarios were designed as multiple convex polygons which were randomly generated in a 2D plane region. Firstly, to verify the effectiveness of the proposed MCR task assignment algorithm, NR = 18 polygonal regions were randomly generated, with all regions distributed in the range of 15 km by 15 km in the 2D map. The coordinates of the corresponding vertices are shown in Table 1 and the distance between each region or base is shown in Appendix A.

Table 1. The coordinates of the corresponding vertices.

No.	Edge Number	Vertex Coordinate Distribution (Counterclockwise)
1	4	(451,2924), (1370,2608), (2172,4206), (651,3428)
2	4	(700,6210), (1208,3942), (2534,5769), (1315,7152)
3	4	(829,10023), (1226,8231), (2510,10965), (1326,11237)
4	4	(978,12231), (2123,12143), (3205,12751), (1890,13917)
5	4	(2205,7910), (3802,7008), (4621,8164), (3386,8481)
6	4	(3134,1465), (5182,1067), (5308,2819), (3641,2613)
7	3	(3602,5501), (4484,4017), (5036,5107)

8	4	(4120,10120), (5429,10231), (5083,12140), (4374,11863)
9	4	(6225,973), (8723,1004), (7128,3125), (6421,3280)
10	4	(6524,8771), (7840,7425), (8361,9310), (6715,9743)
11	4	(7214,12900), (8635,11883), (9054,12710), (8414,14008)
12	5	(8524,7035), (9136,5802), (11100,6359), (10586,8169), (10023,8263)
13	5	(9405,3882), (10224,2411), (11243,3101), (10983,4251), (9815,4180)
14	4	(9930,11196), (10854,9853), (12034,9936), (12034,9936)
15	4	(11804,12421), (13237,12401), (12059,13891), (10926 13452)
16	4	(11708,1206), (13214,1345), (13094,2917), (12181 2458)
17	4	(13180,4424), (13309,3767), (14928,4105), (14841,5606)
18	5	(13142,8175), (13203,6908), (14181,6721), (14900,6927), (14726,7801)

Distributions of the regions are shown in Figure 5. The areas of the regions were different to verify the effectiveness of the algorithm. The Shoelace Algorithm was applied to find the areas of these polygon regions. The smallest area was region 7 with 0.89 km^2 and the largest area was region 12 with 3.96 km^2.

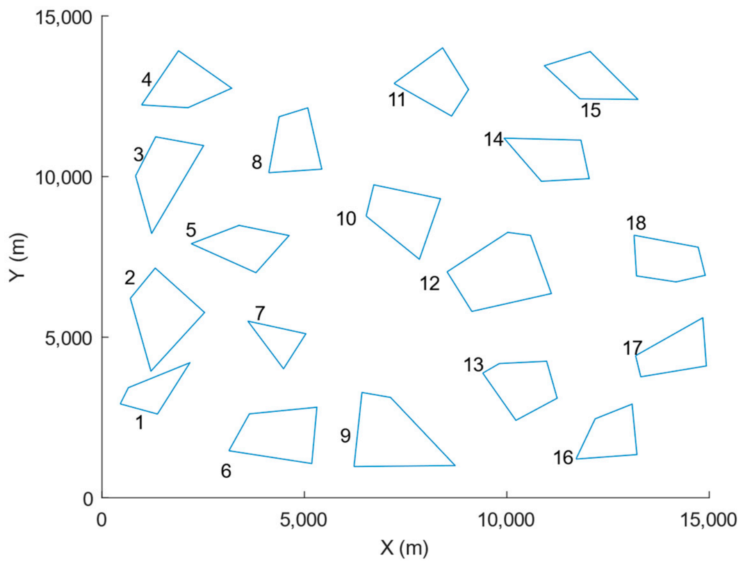

Figure 5. Distribution of the regions.

Three UAVs were used to perform the coverage task. The parameters of the common fixed-wing UAV on the market were found in the related literature [39]. Two sets of UAV parameters were set separately in this study. The performance parameters for homogeneous UAV and heterogeneous UAV are shown in Table 2. Numerical experiments were performed separately for both homogeneous and heterogeneous UAVs in 18 regions.

Table 2. The performance parameters for homogeneous and heterogeneous UAV.

	No.	v (m/s)	w (m)
Homogeneous UAV	UAV1	25	100
	UAV2	25	100
	UAV3	25	100
Heterogeneous UAV	UAV4	20	100
	UAV 5	25	90
	UAV 6	30	110

6. Results and Discussion

The results were compared with three other task allocation algorithms in the same scenario: shortest distance first (SDF), largest area first (LAF) and high effective time rate first (HETRF). SDF assigns the closest area to the UAV each time. LAF allocates the largest area to the UAV each time. HETRF is a new heuristic algorithm to balance the effective time. By analyzing the data results of the MCR assignment algorithm and other task assignment algorithms in detail, the effectiveness, equilibrium and robustness of the proposed MCR assignment algorithm were verified.

6.1. Homogeneous UAVs

The CPP of homogeneous UAVs for four algorithms are shown in Figure 6 and the consumed time is shown in Figure 7. The results of the four algorithms for homogeneous UAVs show significant differences. The three UAV paths assigned by the SDF algorithm have no crossover. However, since the SDF algorithm did not consider the size of the region, the consumed time is restricted by UAV2, which is 109.07 min, ranking the third longest time of the four algorithms. The three UAV paths assigned by the LAF algorithm produce numbers of intersections. The transfer distance is the largest among the four algorithms, and the completion of the task coverage time is 121 min, which is also the longest among the four algorithms. Results by the HETRF are similar to the SDF. However, the regions allocated by UAV1 and UAV2 are not reasonable. This results in a large transfer distance between the regions, particularly the time consumption of UAV2 transfer between regions 7 and 11. Under the MCR allocation algorithm proposed in this study, the three UAV paths do not have any intersection. The mission area and distribution for the UAVs are more reasonable. The time cost for the mission is 103.3, ranking in first place, which is 5.3 min shorter than the HETRF of the second rank.

From the perspective of time consumption, the maximum time costs of SDF, LAF, HETRF and MCR are 109.07 min, 121 min, 108.6 min and 103.03 min, respectively. Compared with the algorithms of SDF, LAF and HETRF, the time consumption for the MCR algorithm is reduced by 5.5%, 14.9% and 5.1%, respectively. The overall variances of the four assignments method are 38.99, 16.17, 19.73 and 1.24, respectively.

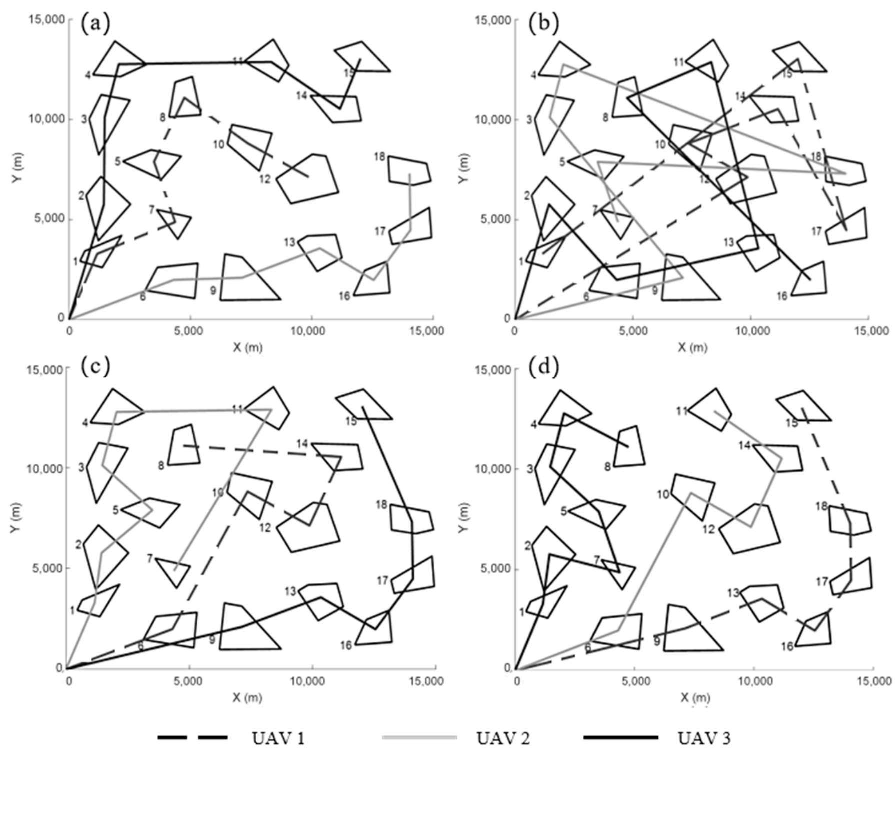

Figure 6. The CPP of homogeneous UAVs for four algorithms: (**a**) SDF, (**b**) LAF, (**c**) HETRF, (**d**) MCR.

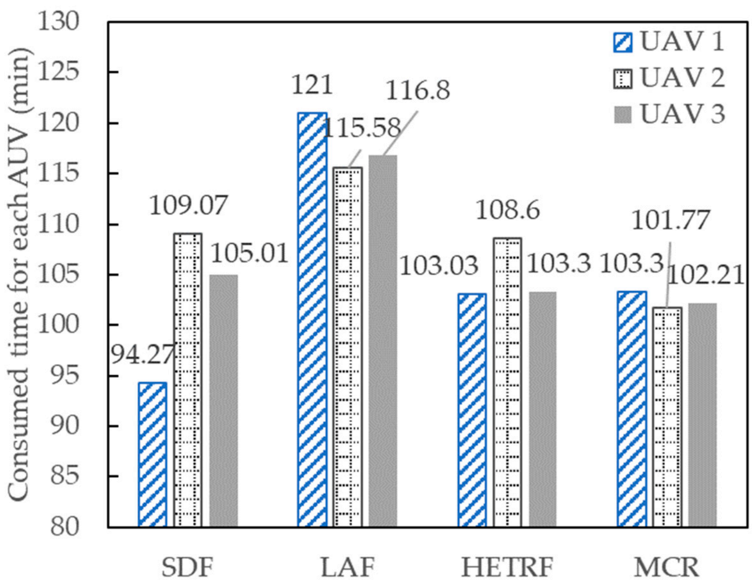

Figure 7. The consumed time of homogeneous UAVs for four algorithms.

6.2. Heterogeneous UAVs

The CPP of heterogeneous UAVs for the four algorithms is shown in Figure 8 and the consumed time is shown in Figure 9. The results of the four algorithms for heterogeneous UAVs also show significant differences. The three UAV paths assigned by the SDF algorithm produce fewer intersections, but the UAV performance and regional area size are not considered. UAV4 has the weakest performance, but under this assignment, it takes 108.97 min to complete the coverage task, much longer than UAV5 and UAV6. For the LAF algorithm, the three UAV paths still have many intersections. The transfer distance is the largest among the four algorithms, and the time consumption of the coverage task is 125.13 min, which is the largest among the four algorithms. In HETRF, UAV5 is assigned more areas, resulting in a longer time to complete the coverage task. The transfer path for UAV6 between region 8 and 18 is unreasonably long, resulting in a significant amount of ineffective time. The three UAV paths assigned by the MCR algorithm do not have any crossover. Either region allocation or coverage sequence is more reasonable. The completion time is the shortest.

The maximum time costs of the SDF, LAF, HETRF and MCR algorithms are 108.97 min, 125.13 min, 107.63 min and 104.29 min, respectively. Compared with the SDF, LAF and HETRF algorithms, the time consumption of the MCR algorithm is reduced by 4.3%, 16.7% and 3%, respectively. The overall variances of the four allocation results are 19.24, 11.21, 7.76 and 1.8, respectively.

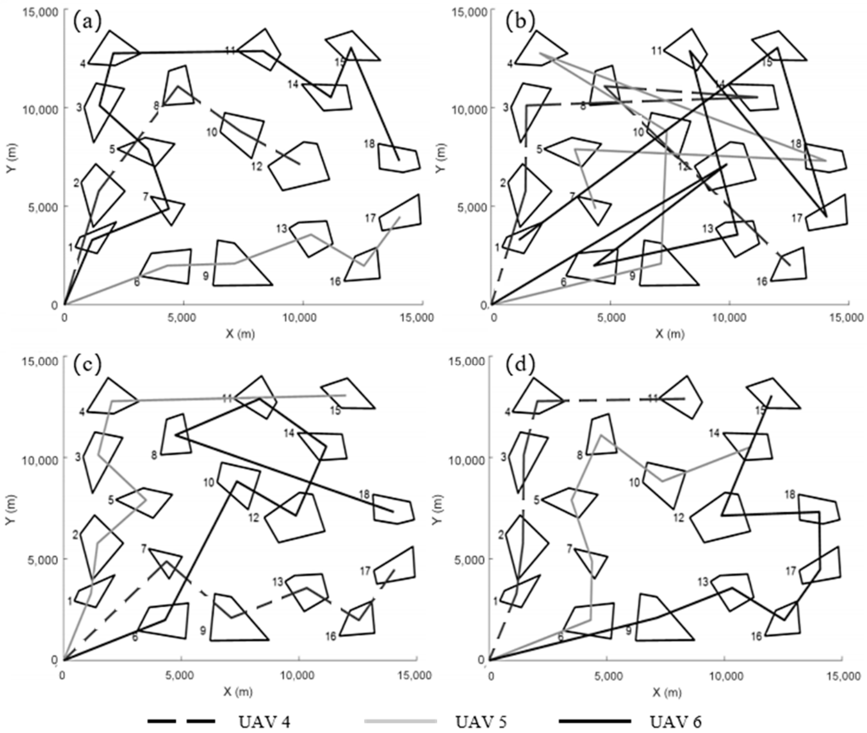

Figure 8. The CPP of heterogeneous UAVs for four algorithms: (**a**) SDF, (**b**) LAF, (**c**) HETRF, (**d**) MCR.

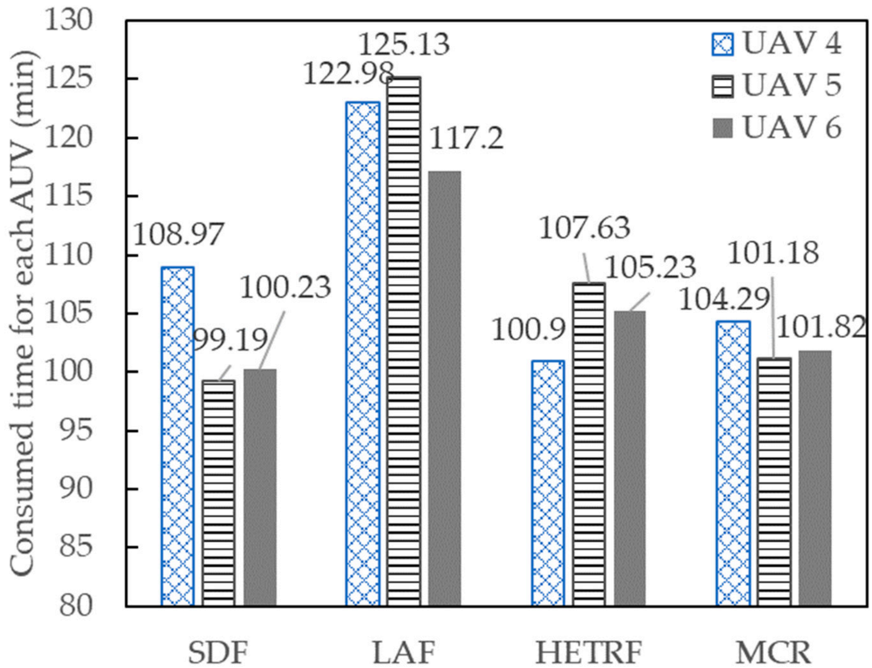

Figure 9. The consumed time of heterogeneous UAVs for four algorithms.

In general, when using the MCR algorithm, the maximum time consumption is the shortest. The time cost for three UAVs has the smallest overall variance and the minimum time consumption differences of the three drones, proving the assigned tasks are well balanced. It shows that the MCR allocation algorithm has better performance for both homogeneous and heterogeneous UAVs.

6.3. Effect of the UAV Number and Region Number

The total number of UAVs is one of the key factors influencing the outcome of full-coverage task assignment when the conditions of the regions are determined. Therefore, two, three, four, five, six, seven and eight UAVs were used in this 18-region experimental scenario to explore the impact of the number of UAVs on the allocation results. Homogeneous UAV parameters were used in this numerical experiment to avoid the impact of UAV parameters on the allocation results. The time consumption for each algorithm is shown in Figure 10. The results demonstrate that the MCR algorithm gives shortest time consumption in all cases.

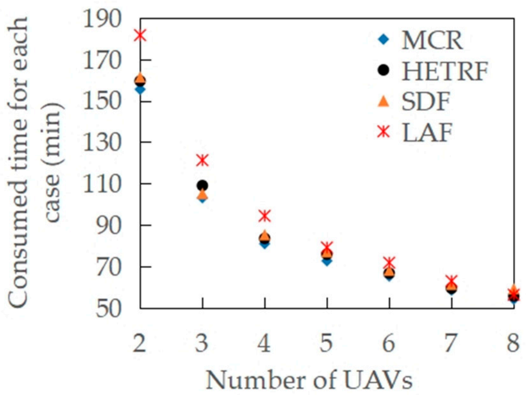

Figure 10. Time consumption changes with the number of drones.

When the number of drones is constant, the number of regions is also one of the factors affecting the results of the algorithm. To further validate the performance of the MCR task assignment algorithm, more sets of data were randomly generated for testing the effect of region number. The number of regions varied from 8 to 24 and the same homogeneous UAV parameters were used. The maximum UAV time consumptions of the four algorithms under each group of regions was recorded, as shown in Figure 11. The results indicate that the MCR algorithm obtains the shortest time in all cases, although HETRF has close performance in 8, 10 and 14 regions.

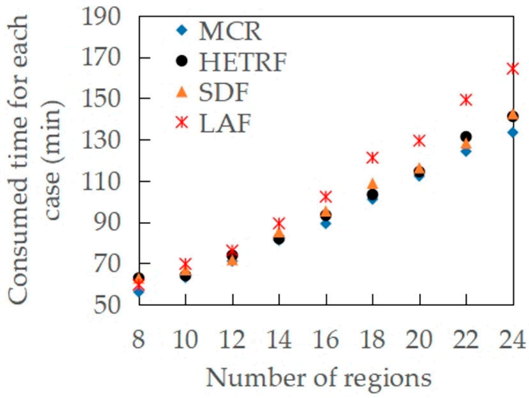

Figure 11. Time consumption changes with the number of regions.

It is worth noting that although the endurance is assumed to meet the requirement, the endurance in reality restricts the total number of the task regions. The endurance of UAVs in this work referenced the HC series of Honeycomb whose endurance is normally 3–8 h. This means, with the increasing of the area and number of regions, UAVs do not have enough fuel or battery capacity to finish the task. However, with some ground transportation, the UAVs can land on the ground vehicle to refuel or recharge, and the vehicles can take UAVs to the next task region [40,41]. This could be a solution to enhance the application of the method proposed in this study.

7. Conclusions

This paper decomposed the multi-UAV coverage multi-region problem into two stages: multi-UAV region allocation and path replanning. In the first stage, the area with priority selection and minimum consumption ratio achieved the relatively equal task pre-allocation for each UAV. The second stage of path replanning was to replan the path of the UAV traversal of each region in the first stage, which improved the coverage efficiency of the UAVs. The MCR-based method for the multi-UAV coverage multi-region problem was verified to be effective using numerical experiments. Even compared with the HETRF algorithm, which was also an advanced CPP algorithm, the time consumption was reduced by 5.1% and 3% for homogeneous and heterogenous UAV performance, respectively. The improvement was also obvious when changing the number of UAVs and regions.

Author Contributions: Conceptualization, J.C.; methodology, R.Z.; software, R.Z.; formal analysis, J.C. and H.Z.; writing—original draft, J.C.; writing—review and editing, H.Z., J.L. and J.H.; supervision, J.C. and J.L.; project administration, J.H. All authors have read and agreed to the published version of the manuscript.

Funding: This work is supported by Changsha Science and Technology Plan (kq2004081). This work is supported by National Key R&D Program of China National Key Research and Development Program (2022YFC3090500). This work is funded by Open Foundation of the State Key Laboratory of Fluid Power and Mechatronic Systems (GZKF-202228).

Data Availability Statement: Data are available from the authors on request.

Acknowledgments: We are grateful for resources from the High-Performance Computing Center of Central South University.

Conflicts of Interest: The authors declare no conflict of interest. The funders had no role in the design of the study; in the collection, analyses, or interpretation of data; in the writing of the manuscript; or in the decision to publish the results.

Nomenclature

$A = \{a_1, a_2, \dots, a_m\}$	corresponding regions areas
$C_{x \to y}$	distance from point x to y.
d_{ij}	distance between any two regions
$D(\mathrm{x}, V')$	the shortest distance from the starting point s, passing all target points in V' once and arriving at x.
h	height of the UAV from the ground
m	number of regions
n	number of UAVs
$R = \{R_1, R_2, \dots, R_m\}$	regions need to be covered
$U = \{U_1, U_2, \dots, U_n\}$	A set of UAVs with different speed and scan camera performance
$U_i = [v_i, w_i]$	performance of UAV i
v_i	speed of the UAV i
V	set of all vertices
w_i	scan width of the UAV i
w_1	rear width of the scan area
w_2	front width of the UAV scanning area
x_{ij}^k, x_j^k	control variables
α	mounting angle of the UAV imaging sensor

β	horizontal field of view angle
γ	vertical field of view angle of the UAV imaging sensor
θ	elevation angle of the UAV
BETR	Balanced Effective Task Rate
CPP	Coverage Path Planning
HETRF	High Effective Time Rate First
MCR	Minimum Consumption Ratio
TSP	travel salesman problem
UAV	unmanned aerial vehicle

Appendix A

Table A1. Distance between each region or base (m).

	Base	1	2	3	4	5	6	7	8	9	10	11	12	13	14	15	16	17	18
Base	0																		
1	3490	0																	
2	5945	2492	0																
3	10,220	6829	4345	0															
4	12,923	9510	7018	2708	0														
5	8633	5161	2960	3011	5082	0													
6	4753	3412	4748	8606	11,005	5955	0												
7	6549	3582	3067	5988	8221	3138	2884	0											
8	12,063	8583	6267	3420	3177	3432	9107	6224	0										
9	7426	6082	6768	9809	11,811	6833	2809	3910	9300	0									
10	11,481	8300	6657	6029	6617	3965	7469	4941	3462	6720	0								
11	15,334	11,967	9898	7391	6281	6937	11,600	8924	3999	10,846	4176	0							
12	12,176	9519	8543	8916	9642	6416	7566	5942	6476	5732	3027	5953	0						
13	10,931	9177	9163	11,018	12,377	8085	6220	6102	9368	3530	6031	9523	3590	0					
14	15,345	12,345	10,826	9698	9381	8100	10,944	8834	6434	9351	4172	3677	3639	7014	0				
15	17,726	14,583	12,828	10,932	9961	9941	13,462	11,177	7513	11,985	6282	3680	6288	9622	2649	0			
16	12,704	11,463	11,737	13,741	15,047	10,804	8232	8672	11,989	5426	8578	11,682	5798	2722	8660	11,073	0		
17	14,759	12,957	12,691	13,796	14,594	11,099	10,059	9698	11,422	7336	7984	10,170	4958	3840	6714	8809	2918	0	
18	15,890	13,537	12,723	12,870	13,144	10,563	11,146	10,009	10,004	8735	6841	7914	4192	5352	4254	5990	5635	2936	0

Appendix B

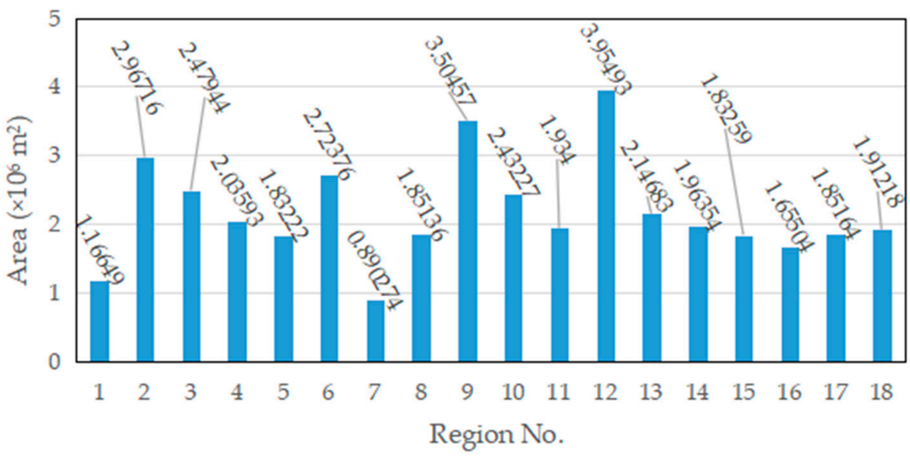

Figure A1. Area of Each Region.

References

1. Park, W.; Lee, K.; Im, K. A Proposal on the Aviation Rules of the Military UAV in the National Airspace System. *J. Korean Soc. Aviat. Aeronaut*. **2014**, *22*, 22–31.
2. Bejiga, M.B.; Zeggada, A.; Nouffidj, A.; Melgani, F. A convolutional neural network approach for assisting avalanche search and rescue operations with UAV imagery. *Remote Sens*. **2017**, *9*, 100.
3. Wang, S.; Han, Y.; Chen, J.; Pan, Y.; Cao, Y.; Meng, H. A Transfer-learning-based Feature Classification Algorithm for UAV Imagery in Crop Risk Management. Desalin. *Water Treat*. **2020**, *181*, 330–337.
4. Ollero, A.; Kondak, K. 10 Years in the Cooperation of Unmanned Aerial Systems. In Proceedings of the IEEE/RSJ International Conference on Intelligent Robots & Systems, Vilamoura-Algarve, Portugal, 7–12 October 2012; IEEE: New York, NY, USA, 2012; pp. 5450–5451.
5. Huang, H.; Savkin, A.V.; Li, X. Reactive autonomous navigation of UAVs for dynamic sensing coverage of mobile ground targets. *Sensors* **2020**, *20*, 3720.
6. Mansouri, S.S.; Kanellakis, C.; Fresk, E.; Kominiak, D.; Nikolakopoulos, G. Cooperative coverage path planning for visual inspection. *Control Eng. Pract.* **2018**, *74*, 118–131.
7. Guo, Y.; Liu, C.; Coombes, M. Spraying Coverage Path Planning for Agriculture Unmanned Aerial Vehicles. In Proceedings of the 26th International Conference on Automation and Computing (ICAC), Portsmouth, England, 2–4 September 2021; IEEE: New York, NY, USA, 2021; pp. 1–6.
8. Wang, C.; Liu, P.; Zhang, T.; Sun, J. The Adaptive Vortex Search Algorithm of Optimal Path Planning for Forest Fire Rescue UAV. In Proceedings of the 2018 IEEE 3rd Advanced Information Technology, Electronic and Automation Control Conference (IAEAC), Chongqing, China, 12–14 October 2018; IEEE: New York, NY, USA, 2018; pp. 400–403.
9. Vazquez-Carmona, E.V.; Vasquez-Gomez, J.I.; Herrera-Lozada, J.C.; Antonio-Cruz, M. Coverage path planning for spraying drones. *Comput. Ind. Eng.* **2022**, *168*, 108125.
10. Maini, P.; Sundar, K.; Singh, M.; Rathinam, S.; Sujit, P.B. Cooperative aerial–ground vehicle route planning with fuel constraints for coverage applications. *IEEE Trans. Aerosp. Electron. Syst.* **2019**, *55*, 3016–3028.
11. Galceran, E.; Carreras, M. A survey on coverage path planning for robotics. *Robot. Auton. Syst.* **2013**, *61*, 1258–1276.
12. Yang, C.H.; Tsai, M.H.; Kang, S.C.; Hung, C.Y. UAV path planning method for digital terrain model reconstruction—A debris fan example. *Autom. Constr.* **2018**, *93*, 214–230.
13. Cabreira, T.M.; Brisolara, L.B.; Paulo, R.F.J. Survey on coverage path planning with unmanned aerial vehicles. *Drones* **2019**, *3*, 4.
14. Ho, Y.-H.; Tsai, Y.-J. Open Collaborative Platform for Multi-Drones to Support Search and Rescue Operations. *Drones* **2022**, *6*, 132.
15. Yuan, J.; Liu, Z.; Lian, Y.; Chen, L.; An, Q.; Wang, L.; Ma, B. Global Optimization of UAV Area Coverage Path Planning Based on Good Point Set and Genetic Algorithm. *Aerospace* **2022**, *9*, 86. https://doi.org/10.3390/aerospace9020086.
16. Shivgan, R.; Dong, Z. Energy-Efficient Drone Coverage Path Planning Using Genetic Algorithm. In Proceedings of the 2020 IEEE 21st International Conference on High Performance Switching and Routing (HPSR), Newark, NJ, USA, 11–14 May 2020; IEEE: New York, NY, USA, 2020; pp. 1–6.
17. Jing, W.; Deng, D.; Wu, Y.; Shimada, K. Multi-uav Coverage Path Planning for the Inspection of Large and Complex Structures. In Proceedings of the 2020 IEEE/RSJ International Conference on Intelligent Robots and Systems (IROS), Las Vegas, NV, USA, 25–29 October 2020; IEEE: New York, NY, USA, 2020; pp. 1480–1486.
18. Wang, J.; Chen, W.; Temu, V. Multi-vehicle motion planning for search and tracking. In Proceedings of the 2018 IEEE conference on multimedia information processing and retrieval (MIPR), Miami, FL, USA, 10–12 April 2018; IEEE: New York, NY, USA, 2018; pp. 352–355.
19. Huang, J.; Fu, W.; Luo, S.; Wang, C.; Zhang, B.; Bai, Y. A Practical Interlacing-Based Coverage Path Planning Method for Fixed-Wing UAV Photogrammetry in Convex Polygon Regions. *Aerospace* **2022**, *9*, 521. https://doi.org/10.3390/aerospace9090521.
20. Valente, J.; Sanz, D.; Del Cerro, J.; Barrientos, A.; de Frutos, M. Near-optimal coverage trajectories for image mosaicing using a mini quad-rotor over irregular-shaped fields. *Precis. Agric.* **2013**, *14*, 115–132.
21. Apuroop, K.G.S.; Le, A.V.; Elara, M.R.; Sheu, B.J. Reinforcement learning-based complete area coverage path planning for a modified hTrihex robot. *Sensors* **2021**, *21*, 1067.
22. Theile, M.; Bayerlein, H.; Nai, R.; Gesbert, D.; Caccamo, M. UAV Coverage Path Planning Under Varying Power Constraints Using Deep Reinforcement Learning. In Proceedings of the 2020 IEEE/RSJ International Conference on Intelligent Robots and Systems (IROS), Las Vegas, NV, USA, 25–29 October 2021; pp. 1444–1449.
23. Wu, Q.; Zhou, S.; Yan, S. Research on multi UAV coverage reconnaissance method in complex area. *Tactical Missile Technol.* **2016**, *1*, 50–55. (In Chinese)
24. Gao, C.; Kou, Y.; Li, Z.; Xu, A.; Li, Y.; Chang, Y. Cooperative coverage path planning for small UAVs. *Syst. Eng. Electron. Technol.* **2019**, *41*, 1294–1299. (In Chinese)
25. Luo, C.; Yang, S. A real-time cooperative sweeping strategy for multiple cleaning robots. In Proceedings of the 2002 IEEE International Symposium on Intelligent Control, Vancouver, Canada, 27–30 October 2002; IEEE: New York, NY, USA, 2002; pp. 660–665.

26. Geiger, B.; Schmidt, E.; Horn, J. Use of neural network approximation in multiple-unmanned aerial vehicle trajectory optimization. In Proceedings of the AIAA Guidance, Navigation, and Control Conference, Chicago, CA, USA, 10–13 August 2009; p. 6103.
27. Applegate, D.L.; Bixby, R.M.; Chvátal, V.; Cook, W.J. The Traveling Salesman Problem. In *The Traveling Salesman Problem*; Princeton University Press: Princeton, NJ, USA, 2011; ISBN 978–0-691–12993–8.
28. Steinerberger, S. New Bounds for the Traveling Salesman Constant. *Adv. Appl. Probab.* **2015**, *47*, 27–36.
29. Yao, J.; Li, X.; Zhang, Y.; Ji, J.; Wang, Y.; Zhang, D.; Liu, Y. Three-Dimensional Path Planning for Unmanned Helicopter Using Memory-Enhanced Dueling Deep Q Network. *Aerospace* **2022**, *9*, 417. https://doi.org/10.3390/aerospace9080417.
30. Koenig, D.; Tsvietkova, A. NP–hard problems naturally arising in knot theory. *T Am. Math. Soc. Ser. B* **2021**, *8*, 420–441.
31. Chen, J.; Ling, F.; Zhang, Y.; You, T.; Liu, Y.; Du, X. Coverage path planning of heterogeneous unmanned aerial vehicles based on ant colony system. *Swarm Evol. Comput.* **2022**, *69*, 101005.
32. Majeed, A.; Hwang, S.O. A Multi-Objective Coverage Path Planning Algorithm for UAVs to Cover Spatially Distributed Regions in Urban Environments. *Aerospace* **2021**, *8*, 343. https://doi.org/10.3390/aerospace8110343.
33. Chen, J.; Du, C.; Lu, X.; Chen, K. Multi-region Coverage Path Planning for Heterogeneous Unmanned Aerial Vehicles Systems. In Proceedings of the 2019 IEEE International Conference on Service-Oriented System Engineering (SOSE), San Francisco East Bay, CA, USA, 4–9 April 2019; IEEE: New York, NY, USA, 2019; 356–361.
34. Xie, J.; Chen, J. Multi-regional coverage path planning for robots with energy constraint. In Proceedings of the 2020 IEEE 16th International Conference on Control & Automation (ICCA), Sapporo, Hokkaido, Japan, 9–11 October 2020; IEEE: New York, NY, USA, 2020; pp. 1372–1377.
35. Yu, X.; Jin, S.; Shi, D. Balanced multi-region coverage path planning for unmanned aerial vehicles. In Proceedings of the 2020 IEEE International Conference on Systems, Man, and Cybernetics (SMC), Toronto, ON, Canada, 11–14 October 2020; IEEE: New York, NY, USA, 2020; pp. 3499–3506.
36. Sundar, K.; Venkatachalam, S.; Rathinam, S. Formulations and algorithms for the multiple depot, fuel-constrained, multiple vehicle routing problem. In Proceedings of the 2016 American Control Conference (ACC), Boston, MA, USA, 6–8 July 2016; IEEE: New York, NY, USA, 2016, 6489–6494.
37. Chen, J.; Du, C.; Zhang, Y.; Han, P.; Wei, W. A clustering-based coverage path planning method for autonomous heterogeneous UAVs. *IEEE Trans. Intell. Transp. Syst*. **2021**, *23*, 25546–25556.
38. Li, J.; Xiong, Y.; She, J.; Wu, M. A path planning method for sweep coverage with multiple UAVs. *IEEE Internet Things J.* **2020**, *7*, 8967–8978.
39. Peng, H.; Shen, L.; Huo, X. Research on Multiple UAV Cooperative Area Coverage Searching (In Chinese). *J. Syst. Simul.* **2007**, *19*, 2472–2476. https://doi.org/10.16182/j.cnki.joss.2007.11.022.
40. Huang, H.; Savkin, A.V. Aerial Surveillance in Cities: When UAVs Take Public Transportation Vehicles. *IEEE Trans. Autom. Sci. Eng (Early Access)*. 2022, 1-12. https://doi.org/10.1109/TASE.2022.3182057.
41. Yu, K.; O'Kane, J.M.; Tokekar, P. Coverage of an Environment Using Energy-Constrained Unmanned Aerial Vehicles. In Proceedings of the 2019 International Conference on Robotics and Automation (ICRA), Montreal, Canada, 20–24 May 2019; IEEE: New York, NY, USA, 2019; pp. 3259–3265.